

Shock wave structure in gas mixtures with large mass disparity

By R. FERNÁNDEZ-FERIA
AND J. FERNÁNDEZ DE LA MORA

Mechanical Engineering Department, Yale University, Box 2159 YS New Haven,
CT 06520, USA

(Received 2 December 1985)

The structure of normal shock waves is considered when the ratio of molecular masses m_p/m of a binary mixture of inert monatomic gases is large and the density ratio ρ_p/ρ is of order unity or below. Generalized hydrodynamic equations, valid for arbitrary intermolecular potentials, are obtained from a hypersonic closure of the kinetic equation for the heavy gas and a near-equilibrium closure for the light component. Because the Prandtl number of the light gas and the Schmidt number of the mixture are nearly constant, the only independent transport coefficient arising in the model is the viscosity μ of the light gas, which is absorbed into a new independent position variable s . Knowledge of μ as a function of temperature thus determines the shock structure independently from the details of the intermolecular potential, allowing comparison with experiments in the complete absence of free parameters. In terms of the ratio M (frozen Mach number) between the speed of propagation and the sound speed of the light gas in the unperturbed medium, one finds that: (i) When $M > 1$, the behaviour is similar to that of a 'dusty gas', with a broad relaxation layer (outer solution) following a sharp boundary layer through which the speed of the heavy gas is almost constant (a shock within a shock). (ii) When $(1 + \rho_p/\rho)^{-1/2} < M < 1$, the boundary layer disappears, yielding a so-called 'fully dispersed wave'. (iii) Because the internal energy of the heavy gas is negligible, the present problem differs from previous shock studies in that, for the first time, the structure of the relaxation region is obtained algebraically in phase space, thus permitting an exhaustive study of the behaviour. From it, the overshooting solution found by Sherman (1960) is related to the unphysical degenerate branch of the outer solution arising when $M > 1$, showing a failure of the Chapman–Enskog theory, even for weak shocks, when the heavy gas is dilute. Also, an algebraic explanation arises for the 'double hump structure' observed in He–Xe shocks. (iv) When M is nearly unity, the initial boundary layer spreads out, and the structure must be obtained by integration of a numerically unstable system of three differential equations. However, the reduction of order brought about by the weak variation of the light-gas entropy at the head of the shock, results in a stable system of equations that we integrate numerically. Excellent phase-space agreement with recent shock-tube experiments of Tarczynski, Herczynski & Walenta (1986) is found for both weak and strong shocks.

1. Introduction

The structure of normal shock waves in binary gas mixtures has been studied since the work of Cowling (1942), who considered the inter-diffusion of both species as

the only dissipative mechanism present. The inclusion of viscosity and thermal conductivity within the framework of the Chapman–Enskog (C–E) theory was done by Dyakov (1954) and Sherman (1960). Sherman predicted an overshoot of the heavy-species velocity in the limit of large mass ratio and small molar fraction of the heavy component. This overshoot was not observed in experiments with Ar–He mixtures made by Center (1967) nor in numerical simulations using the Monte Carlo Method (Bird 1968, 1984). Goldman & Sirovich (1969) used an approach more general than the C–E theory (Goldman & Sirovich 1967), allowing for temperature and velocity differences between the two species. Although their system of four governing differential equations was numerically unstable (Sirovich & Goldman 1969), Goldman & Sirovich (1969) studied in detail the limit of weak shocks without ever encountering any velocity overshoot. Harris & Bienkowski (1971), using the moment method of kinetic theory for Maxwellian molecules, developed the most complete available hydrodynamic theory, valid also for strong shock waves. They analysed the resulting equations for a broad range of asymptotic limits of the molecular mass ratio m/m_p (subscript p corresponds to the heavy species) and the density ratio upstream of the shock, $\epsilon = (\rho_p/\rho)_{-\infty}$. Relatively recent experiments by Gmurczyk, Tarczyński & Walenta (1979) and Tarczyński *et al.* (1986) with He–Xe mixtures have renewed the interest in the problem owing, partly, to the double-hump structure observed on the light-gas density, characterized by the presence of an intermediate inflexion point. Platkowski (1979) studied the problem through the WKG method but did not find the above structure, which has been obtained by Bratos & Herczyński (1980, 1983) by a combination of a variational approach to the Boltzmann equation and a Monte Carlo calculation of some of the terms occurring in their formulation.

In the present work we consider binary mixtures of inert monatomic gases in the interesting limit $m/m_p \ll 1$ and $\epsilon \leq O(1)$ in which the most peculiar structures have been observed and predicted. Although Harris & Bienkowski (1971) have previously made considerable progress, our analysis of this limit is more exhaustive, is based on fully specified governing equations not restricted to Maxwell molecules and will be enriched by the newly available experiments in He–Xe mixtures. We are also guided by the heavy-molecule–aerosol analogy, first suggested by Reis & Fenn (1963) and successfully exploited in a variety of situations involving gas mixtures with disparate masses (see, e.g. Maise & Fenn 1972; Thuan & Andres 1979; Schwartz & Andres 1977; Fernández de la Mora 1984; Fernández de la Mora, Wilson & Halpern 1984).

We use a hypersonic closure for the conservation equations of the heavy species. This approach is justified when m_p is sufficiently large that the thermal speed of the heavy gas is small compared to the mean mixture speed even downstream of the shock (where, obviously, the mixture is subsonic). The relatively simple resulting equations are solved asymptotically by an expansion in the mass ratio, and the solution has the following features: when the incident frozen Mach number (M) based on the pure light-gas sound speed is less than one but larger than $(1+\epsilon)^{-1/2}$ we find an algebraic solution in phase space valid, in first approximation in the mass ratio, over all the shock wave, and reducing the solution in physical space to a quadrature. When M is larger than one, this algebraic solution is not uniformly valid through all the shock and there is a thin boundary layer (inner region) across which, in first approximation, the velocity of the heavy species remains constant and the light gas is compressed as in a normal shock wave of a pure gas. This situation does not remain valid as M approaches unity because the inner region becomes much thicker. However, in this

case, an additional simplification arises from the fact that the light-gas entropy in the inner region is approximately conserved.

Similar results have been found for shock waves in dusty gases. Carrier (1958) considered two regions: a gas shock assumed as a discontinuity (he neglected the viscosity and thermal conductivity of the gas), and a relaxation zone whose structure is obtained by solving a first-order differential equation in phase space and performing a quadrature in real space. Studies of the relaxation zone were also made by other authors (see Marble 1970, and references therein), in addition to other works including the effect of the volume fraction of particles (see, e.g. Srivastava & Sharma 1982). Hamad & Frohn (1980) included in their analysis the viscosity and thermal conductivity of the gas and the particle volume fraction, obtaining a power expansion solution in phase space for weak shocks (fully dispersed shocks).

The light-gas discontinuity upstream of a broader relaxation region obtained in these 'dusty gas' studies is closely related to some of the structures observed experimentally by Gmurczyk *et al.* (1979) and Tarczynski *et al.* (1986) in He–Xe mixtures. Moreover, the qualitative structure of the shock for the dusty gas given by Hamad & Frohn (1980) is similar to our results and those of Harris & Bienkowski (1971): there is a 'fully dispersed wave' when $M_{\min}^2 < M^2 < 1$ ($M_{\min}^2 = (1 + \epsilon)^{-1}$ in the heavy-molecule case) and an inner region when $M > 1$, which can be considered as a discontinuity with respect to the relaxation zone when $|M - 1|$ is not very small. The present problem is simpler than its dusty-gas analogue because of the negligible role played by the heavy-species internal energy (§2). This feature eliminates the temperature of the heavy gas from the picture, turning the dusty-gas relaxation differential equations into purely algebraic relations (§3.1). Appropriate exploitation of this simplifying feature provides a very complete description of the possible regimes, including an algebraic explanation of the double-hump structures observed (§3.1) and of Sherman's overshooting paradox (§3.2). Another novelty of the present analysis is in the treatment of the region where $M \approx 1$ (§3.3). Our phase-space results are universal in the sense that they do not depend on the form of the interaction potential; only on the mass ratio parameter F (equation (13)), the density ratio ϵ and the Mach number M . They yield excellent agreement with the experiments of Tarczynski *et al.* (1986) for He–Xe mixtures (§5). Knowledge of just the temperature dependence of the viscosity coefficient of the pure light gas allows a fitting-parameter-free conversion of phase-space results into real-space structures which have been shown by Riesco-Chueca *et al.* (1986) to agree rather well with earlier experiments of Gmurczyk *et al.* (1979). Finally, we wish to remark that the present hypersonic results may be extended to higher orders in the mass ratio m/m_p .

2. Governing equations

The integrated one-dimensional and steady conservation equations for species mass, momentum and energy of the mixture can be written as

$$\rho u = \dot{m}. \quad (1)$$

$$\rho_p u_p = \epsilon \dot{m}, \quad (2)$$

$$\rho u^2 + \rho_p u_p^2 + P_{xx} + P_{p,xx} = P, \quad (3)$$

$$\rho u \left(\frac{1}{2} u^2 + e \right) + \rho_p u_p \left(\frac{1}{2} u_p^2 + e_p \right) + u P_{xx} + u_p P_{p,xx} + Q_x + Q_{p,x} = E, \quad (4)$$

where ρ and ρ_p are the densities (subscript p stands for the heavy species); u and u_p the mean velocities; e and e_p the internal energies; P_{xx} and P_{pxx} the xx -component of the pressure tensors; Q_x and Q_{px} the x -components of the heat fluxes; m , P and E are integration constants and ϵ is the density ratio upstream of the shock.

In first approximation in the mass ratio m/m_p , we can write† (Fernández de la Mora & Fernández-Feria 1987)

$$P_{xx} = \frac{\rho}{m} kT - \frac{4}{3}\mu \frac{du}{dx}, \quad (5a)$$

$$Q_x = -\lambda \frac{dT}{dx}, \quad (5b)$$

$$e = \frac{1}{\gamma-1} \frac{k}{m} T, \quad (5c)$$

where T is the light-gas temperature and μ , λ and γ ($\frac{5}{3}$) are the viscosity, thermal conductivity and specific heat ratio of the light gas. Since the density ratio ρ_p/ρ is of order unity, then provided T_p/T remains of order unity inside the shock, P_{pxx}/P_{xx} , Q_{px}/Q_x and e_p/e are quantities of the order of the mass ratio m/m_p (or less) and can be neglected, in first approximation, in (1)–(4). This feature, together with the hypersonic closure (see below), leads to the absence of the heavy-gas temperature from the first-order equations.

The momentum conservation equation for the heavy species can be written as

$$\frac{d}{dx}(\rho_p u_p^2) + \frac{d}{dx}(P_{pxx}) = -\rho_p b_x, \quad (6)$$

where b_x is the x -component of the momentum transfer between both species. As mentioned above, the heavy particles remain in hypersonic conditions across the shock and their pressure tensor is negligible compared to $\rho_p u_p^2$ (hypersonic closure). Moreover, we are going to assume that the slip velocity $u_p - u$ is small compared to the light-gas thermal speed $(2kT/m)^{\frac{1}{2}}$ and the momentum transfer term b_x can be approximated by a linear function of $u_p - u$ (see e.g. Burgers 1969):

$$b_x = \frac{u_p - u}{\tau}, \quad (7)$$

where τ is the momentum relaxation time which can be related to the mixture diffusion coefficient D by the Einstein law $D = kT\tau/m_p$. Thus, (6) can be written as

$$\frac{d}{dx}(\rho_p u_p^2) = -\rho_p \frac{u_p - u}{\tau}. \quad (8)$$

The system of (1)–(5) and (8) is closed in the variables ρ , ρ_p , u , u_p and T . Note that this is so even if the assumption of small slip velocity (7) is replaced by a more general expression for b_x (Riesco-Chueca *et al.* 1986, 1987). The boundary conditions are

$$\rho = \rho_{-\infty}, \quad \rho_p = \epsilon \rho_{-\infty}, \quad u = u_p = u_{-\infty}, \quad T = T_{-\infty} \quad \text{as } x \rightarrow -\infty. \quad (9a)$$

† Actually, the collisions of the light gas with the heavy particles must modify this 'pure light gas' behaviour. But the corrections are of the order of the ratio of number densities, that is, of order $m\epsilon/m_p$, which may be neglected in first approximation. Furthermore, the near-equilibrium closure (for the light gas) implied by (5) requires that the shock-wave width be large compared to the light-gas mean-free-path. This seems to restrict the validity of the present theory to the case of weak shocks, but this is not really the case, as discussed in §4.

far upstream, while the downstream equilibrium conditions are given by the Rankine-Hugoniot relations together with the no-slip condition $u = u_p$.

$$\rho = \rho_\infty, \quad \rho_p = \epsilon \rho_\infty, \quad u = u_p = u_\infty, \quad T = T_\infty \quad \text{as } x \rightarrow +\infty. \quad (9b)$$

Using (9a) to evaluate the integration constants P and E , and in terms of the dimensionless variables

$$\eta = \frac{u}{u_\infty}, \quad \xi = \frac{u_p}{u_\infty}, \quad \theta = \frac{T}{T_\infty}, \quad ds = \frac{3}{4} \frac{\dot{m}}{\mu} dx, \quad (10)$$

(1)–(5) and (8) become

$$\frac{d\eta}{ds} = \eta - 1 + \epsilon(\xi - 1) + \frac{1}{\gamma M^2} \left(\frac{\theta}{\eta} - 1 \right), \quad (11a)$$

$$\begin{aligned} \frac{3}{2Pr(\gamma-1)M^2} \frac{d\theta}{ds} = & -(\eta-1)^2 + \epsilon(\xi-2\eta+1)(\xi-1) \\ & + \frac{2}{\gamma(\gamma-1)M^2} [\theta + (\gamma-1)\eta - \gamma], \end{aligned} \quad (11b)$$

$$F\eta\xi\theta^{-1} \frac{d\xi}{ds} = \eta - \xi, \quad (11c)$$

where the frozen Mach number and the Prandtl number are

$$M = \frac{u_\infty}{(\gamma k T_\infty / m)^{1/2}}, \quad (12a)$$

$$Pr = \frac{\mu}{\lambda} \frac{\gamma}{\gamma-1} \frac{k}{m}. \quad (12b)$$

The Mach number (12a) is the light-gas Mach number or frozen Mach number in the upstream conditions. The mixture Mach number or equilibrium Mach number M_e can be related to M by $M_e^2 = M^2(1+\epsilon)/(1+m\epsilon/m_p)$, or in first approximation in m/m_p , by $M_e^2 = M^2(1+\epsilon)$. The dimensionless parameter F appearing in (11c) is the large quantity

$$F = \frac{3}{4} \gamma \frac{m_p}{m} \frac{M^2}{Sc}, \quad (13)$$

where Sc is the Schmidt number $Sc = \mu/\rho D$. Since Pr and Sc vary very weakly with temperature (Srivastava & Rosner 1979), both have been treated as constants given by their upstream values. Note that when $\epsilon = 0$, (11a) and (11b) are not coupled to (11c) and correspond to the equations for a (weak) shock wave of the light gas as a pure gas (Millán 1975). Equation (11c), though coupled to the hydrodynamical equations (11a) and (11b), is a deterministic equation analogous to the one governing the evolution of the particles in a 'dusty-gas' (Marble 1970).

A feature worth noticing in the governing equations (11) is their universality, or independence from the particular details of the intermolecular interaction. The solution in s -space feels the microscopic features of the system only through the group Sc absorbed into the mass ratio parameter F ($Pr = \frac{3}{4}$ for a monatomic gas). The real (x)-space shock structure does depend on the interaction potential of the pure light gas, but only through its viscosity coefficient μ (equation (10d)).

3. Solution

Eliminating ds , (11) can be written in phase space (η, ξ, θ) as

$$\frac{(\eta - \xi)\theta}{\eta\xi} \frac{1}{F} \frac{d\eta}{d\xi} = \eta - 1 + \epsilon(\xi - 1) + \frac{1}{\gamma M^2} \left(\frac{\theta}{\eta} - 1 \right). \quad (14a)$$

$$\begin{aligned} \frac{(\eta - \xi)\theta}{\eta\xi} \frac{3}{2P_r(\gamma - 1)M^2} \frac{1}{F} \frac{d\theta}{d\xi} = & -(\eta - 1)^2 + \epsilon(\xi - 1)(\xi - 2\eta + 1) \\ & + \frac{2}{\gamma(\gamma - 1)M^2} [\theta + (\gamma - 1)\eta - \gamma]. \end{aligned} \quad (14b)$$

The particular solution in which we are interested starts at the singular (fixed) point

$$\eta_1 = \xi_1 = \theta_1 = 1. \quad (15a)$$

and finishes at the second singular (fixed) point at which the right-hand sides of (14) vanish and $\eta = \xi$ (equilibrium conditions)

$$\begin{aligned} \eta_2 = \xi_2 = & \frac{(1 + \epsilon)M^2(\gamma - 1) + 2}{(1 + \epsilon)(\gamma + 1)M^2}, \\ \theta_2 = 1 + & \frac{2(\gamma - 1)}{(\gamma + 1)^2(1 + \epsilon)M^2} [M^2(1 + \epsilon) - 1][\gamma M^2(1 + \epsilon) + 1]. \end{aligned} \quad (15b)$$

The separation between these two fixed points gives the jump across the shock (Rankine-Hugoniot relations).

3.1. Outer solution

The parameter F appearing in (13) is a measure of the two widely different microscopic scales of relaxation occurring in the problem. Its large value permits an asymptotic analysis of (14). In first approximation the left-hand sides can be neglected yielding two algebraic expressions from which θ and η can be written in terms of ξ as the two hyperbolae:

$$\eta = 1 + \frac{1}{\gamma + 1} \left\{ \frac{1 - M^2}{M^2} - \gamma\epsilon(\xi - 1) \mp \left[\left(\frac{1 - M^2}{M^2} - \gamma\epsilon(\xi - 1) \right)^2 + (\gamma + 1)(\epsilon(\gamma - 1)(\xi - 1)^2 - 2\epsilon(\xi - 1)) \right]^{\frac{1}{2}} \right\}. \quad (16a)$$

$$\theta = \eta - \gamma M^2 \eta [\eta - 1 + \epsilon(\xi - 1)]. \quad (16b)$$

Since the higher-order derivatives have been neglected in the differential equations, the above may be called the 'outer' solution, and it may have to be complemented with a boundary layer in the upstream region.

The fact that the (phase-space) structure of these shock waves may be given analytically is a remarkable feature of the present problem which has no precedent in the field†. As a rule, the shock structure is determined by numerical integration of a relaxation equation. The reduction of our system to an algebraic one is due to

† Although (51a, b) of Harris & Bienkowski (1971) are equivalent to (16a, b) above, these authors do not unfold the physical implications that follow from them.

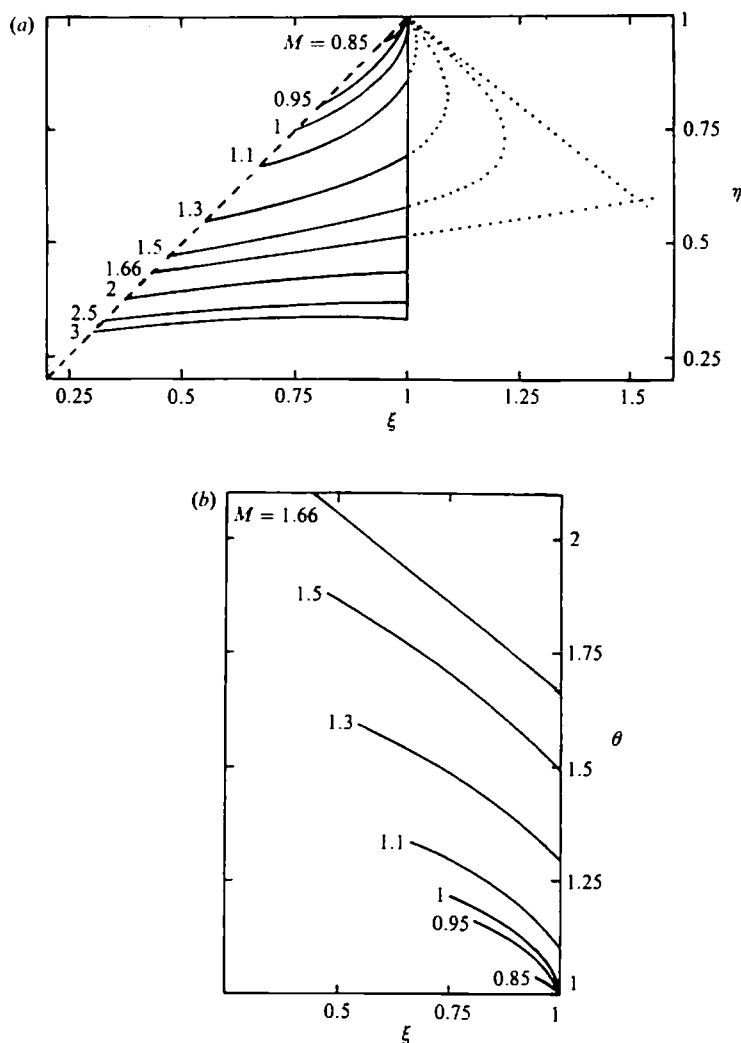


FIGURE 1. Phase-space outer solution [equations (16)] for a He-Xe mixture with $\epsilon = 0.5$ and different values of the upstream frozen Mach number M .

the absence of the heavy-species temperature from the picture. We may thus explore trivially the effect of the various parameters of the problem, M , ϵ , etc.

The outer solution given by (16) is represented in figure 1 for different Mach numbers. Notice that when the frozen Mach number is less than one and the equilibrium Mach number is larger than one (that is, in the range $[1 + \epsilon]^{-1/2} < M < 1$), this outer solution is uniformly valid through all the shock (fully dispersed wave). When $M = 1$, the hyperbolae have an infinite slope at $\xi = 1$, and when $M > 1$ the initial slopes are negative. For M in the range $1 < M < M_*$, where M_* is given by

$$\frac{1 - M_*^2}{M_*^2} = \frac{-\epsilon(\gamma + 1)}{\gamma\epsilon + [\gamma^2\epsilon(1 + \epsilon) - \epsilon]^2},$$

the solution (16) satisfies both boundary conditions, but at the expense of a physically impossible overshoot (analogous to Sherman's) into the region $\xi > 1$. Therefore, when

$M > 1$, the outer solution is only valid for $\xi < 1$ and a discontinuity appears at $\xi = 1$. Actually, this discontinuity corresponds to the light-gas shock wave as a pure gas since the intersections of (16) with $\xi = 1$ are

$$\eta_1 = \frac{M^2(\gamma-1)+2}{(\gamma+1)M^2} \quad (15')$$

$$\theta_1 = 1 + \frac{2(\gamma-1)}{(\gamma+1)^2 M^2} (M^2-1)(\gamma M^2+1) \quad (15'')$$

which give the Rankine-Hugoniot relations for a pure gas. For $M = M_*$, the hyperbolae (equation (16)) became degenerate and the outer solutions are straight lines:

$$\eta = \frac{M^2(\gamma-1)+2}{(\gamma+1)M^2} + \frac{\epsilon}{(1+\epsilon)M^2-1} (\xi-1),$$

$$\theta = 1 + \frac{2(\gamma-1)}{(\gamma+1)^2 M^2} (M^2-1)(\gamma M^2+1) + \frac{(\gamma-1)\epsilon[M^4(1+\epsilon)\gamma+1]}{(\gamma+1)[1-(1+\epsilon)M^2]} (\xi-1).$$

When $M \geq M_*$ the outer solution is also valid only for $\xi < 1$, but no longer passes through the downstream equilibrium point. It would thus fail in giving the shock structure, even if one were willing to accept the overshooting solutions as physically meaningful!

Another interesting feature of the outer solution is that the light-gas velocity η is not a monotonic function of ξ , but displays a maximum when $M^2 > (2\gamma/[\gamma-1])$. The slow variation of η characterizing the beginning of the relaxation zone in a broad region of Mach numbers starting somewhere below $M = (2\gamma/[\gamma-1])^{1/2} = 5^{1/2}$, leads to a double-hump structure in the light-gas density, in agreement with earlier experimental observations by Gmurczyk *et al.* (1979). The first hump corresponds to the light-gas shock wave, and the second one is contained within the outer solution for Mach numbers M larger than a certain value. This phenomenon is illustrated in figure 2, where η^{-1} (which from (1) is proportional to ρ) given by the outer solution is plotted versus s (making use of (11c)). The necessary condition for the double hump is the existence of an intermediate inflexion point in the relaxation portion of the curve $\eta^{-1}(x)$. This condition would yield the Mach number above which such a double-hump structure exists which, in general, is a function of ϵ and the gas properties. A very rough estimate is given by the condition that $d\eta^{-1}/ds = 0$ at $\xi = 1$, that is, $M^2 = 2\gamma/[\gamma-1]$ (corresponding to $5^{1/2}$ in figure 2). The actual value is always below this.

From the above considerations we conclude that, when the frozen Mach number is larger than one, there is a boundary layer of thickness of order F^{-1} in the neighbourhood of $\xi = 1$ in which right- and left-hand sides of (14) are of the same order and the outer solution is not valid. In first approximation the solution is described in terms of two different regions: a very thin one where the light gas behaves as in a shock wave of a pure gas with the heavy gas 'frozen' ($\xi \approx \text{constant} = 1$), and a zone of relaxation towards the equilibrium state (15b), where the outer solution is valid in first approximation.

3.2. Analysis of the singular points, stability and Sherman's overshoot

The structure of the boundary layer (shock within a shock) must be obtained by numerical integration of the equations. In order to start the integration, it is essential

at $\xi = 1$.
pure gas

(15')

(15'')

M_* , the
straight

).

er passes
he shock
hysically

ocity η is
- 1]). The

a broad
leads to

er experi-
ds to the
lution for

l in figure
is plotted

mp is the
the curve

ble-hump
s. A very

that is,
ays below

h number
-1 in the

the same
olution is

s behaves
tant = 1),

er solution

ot

tained by
s essential

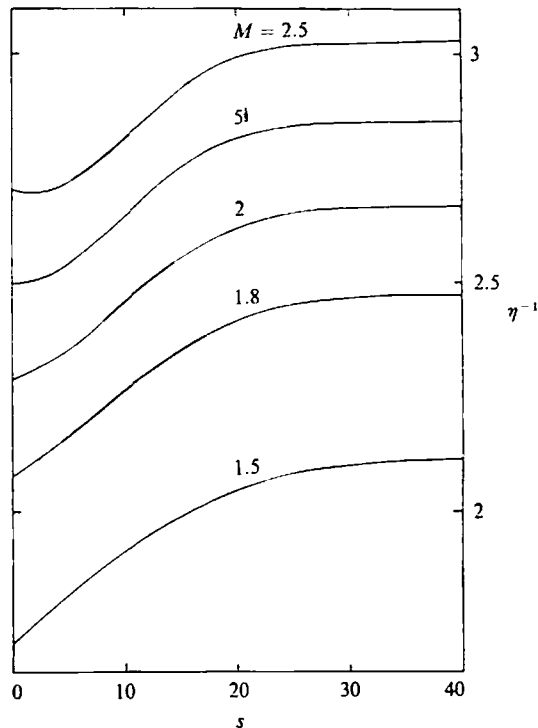


FIGURE 2. Space outer solution for η^{-1} (proportional to the light-gas density). He-Xe, $\epsilon = 0.5$ and $M = 1.5, 1.8, 2, 2.236, 2.5$.

to study the structure of the singular points. Such an analysis will reveal the numerical instability of the system and will complete our explanation of Sherman's paradox. It is also the basis for §3.3.

It must be noticed that, though we have non-dimensionalized the equations with respect to the upstream conditions, the following analysis for the singular point $\theta = \xi = \eta = 1$ is also valid for the downstream singular point because the equations would remain identical if the non-dimensionalization of (10) had been made in terms of the downstream conditions: but in this case, obviously, $M < (1 + \epsilon)^{-1/2}$ would be the downstream Mach number. Linearizing (11) around the singular point $\theta = \xi = \eta = 1$, the characteristic equation for the eigenvalues λ may be written as

$$-(F\lambda + 1) \begin{vmatrix} 1 - \frac{1}{\gamma M^2} - \lambda & \frac{1}{\gamma M^2} \\ \sigma(\gamma - 1) & \sigma - \lambda \end{vmatrix} - \epsilon(\sigma - \lambda) = 0, \quad (17a)$$

where $\sigma = \frac{4}{3}Pr/\gamma$. This equation gives three eigenvalues and, thus, three possible starting directions of the solution. It can be seen that when $(M^2 - 1)/M^2 \gg F^{-1}$ (upstream point), two of the eigenvalues are given, in first approximation in F^{-1} , by equating to zero the determinant of the first term of (17a), coinciding with the eigenvalues for the shock wave of the light gas as a pure gas (Millán 1975):

$$\lambda_1 \lambda_2 = \sigma \left(\frac{M^2 - 1}{M^2} \right) + O(F^{-1}), \quad (17b)$$

$$\lambda_1 + \lambda_2 = \sigma + 1 - \frac{1}{\gamma M^2} + O(F^{-1}). \quad (17c)$$

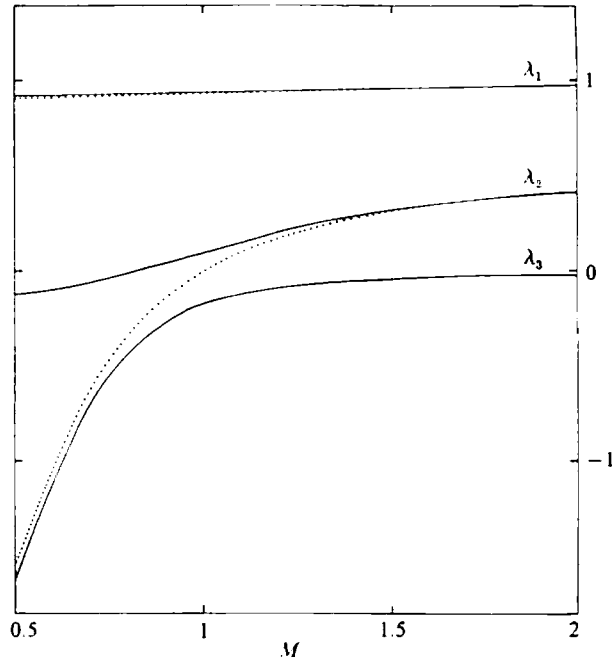


FIGURE 3. Eigenvalues (roots of (17a)) vs. M for a He-Xe mixture with $\epsilon = 0.5$. The broken curves correspond to the pure light gas (He).

The third eigenvalue is a property of the mixture and not of the light gas. It is of order F^{-1} and, in first approximation, is given by

$$\lambda_3 = -\frac{1}{F} \left(1 + \frac{\epsilon M^2}{M^2 - 1} \right) + O(F^{-2}). \quad (17d)$$

The eigenvalues λ_1 and λ_2 yield starting slopes of order F (boundary-layer thickness of order F^{-1}):

$$\left. \frac{d\eta}{d\xi} \right|_{\xi=1} = 1 + \lambda_i F, \quad (18a)$$

$$\left. \frac{d\theta}{d\xi} \right|_{\xi=1} = [1 + \gamma M^2 (\lambda_i - 1)] (1 + \lambda_i F) - \epsilon \gamma M^2 \quad (i = 1, 2). \quad (18b)$$

Since λ_3 is negative, the solution cannot start with this eigenvalue. The initial slopes associated with λ_3 are

$$\left. \frac{d\eta}{d\xi} \right|_{\xi=1} = \frac{\epsilon M^2}{1 - M^2}. \quad (18c)$$

$$\left. \frac{d\theta}{d\eta} \right|_{\eta=1} = 1 - \gamma - \frac{\gamma M^2}{F} \left(1 + \frac{\epsilon M^2}{M^2 - 1} \right) \approx 1 - \gamma. \quad (18d)$$

As pointed out before, the above expressions are also valid for the eigenvalues at the downstream singular point, provided $|M^2 - 1|/M^2 \gg F^{-1}$. For $|M^2 - 1| = O(F^{-1/2})$ or

smaller (17a) can, in first approximation, be written as $\lambda^3 + (\gamma^{-1} - \sigma - 1)\lambda^2 = 0$, yielding an eigenvalue of order unity,

$$\lambda_1 = \sigma + 1 - \frac{1}{\gamma}, \tag{19a}$$

and the other two of order $F^{-\frac{1}{2}}$, given in first approximation by the roots of the equation $\lambda_1 F\lambda^2 + [\lambda_1 \epsilon - \sigma(M^2 - 1)F]\lambda - \epsilon\sigma = 0$. In particular, for $|M^2 - 1| = O(F^{-1})$, one obtains

$$\lambda_{2,3} = \pm \left[\frac{1}{F} \frac{\sigma\epsilon}{\lambda_1} \right]^{\frac{1}{2}}. \tag{19b}$$

The eigenvalues calculated by solving exactly (17a) for a particular case are plotted in figure 3 as a function of the Mach number. For $M > (1 + \epsilon)^{-\frac{1}{2}}$ this figure depicts the behaviour at the upstream singular point, and for $M < (1 + \epsilon)^{-\frac{1}{2}}$ it corresponds to downstream conditions. Note that for $M < (1 + \epsilon)^{-\frac{1}{2}}$ the expression for λ_2 , the eigenvalue that changes its sign at the sonic point $M = (1 + \epsilon)^{-\frac{1}{2}}$, is interchanged with the expression for λ_3 in (17). It has already been seen that the solution cannot start with the negative eigenvalue λ_3 . Also, as in the pure-gas case, it cannot start with the largest eigenvalue λ_1 , which corresponds to a non-physical behaviour incompatible with (5a, b) for the light gas. Therefore, the correct starting (and arriving) eigenvalue is λ_2 , that changes its sign at the sonic point. At the arrival, λ_2 is given by the expression (17d) and corresponds, obviously, to the outer solution.

The eigenvalues corresponding to the pure light gas are also plotted in figure 3. It is observed that, except for a narrow region around $M = 1$, the physically relevant eigenvalue of the light gas almost coincides with λ_2 for $M < 1$, and with λ_3 for $M > 1$. Near $M = 1$ there is a 'bifurcation' in which the modes λ_2 and λ_3 of the mixture interchange their characters, λ_2 being the near null eigenvalue for $M < 1$ and λ_3 taking its role for $M > 1$.

The fact that the eigenvalue λ_2 is neither the largest nor the smallest one, makes the numerical integration unstable. However, from the above analysis, when $(M^2 - 1)/M^2 \gg F^{-\frac{1}{2}}$, the boundary-layer thickness is of order F^{-1} , and, thus, the outer solution for the relaxation zone matched to a boundary layer at $\xi = 1$ (a shock wave for the pure light gas) is a solution with errors of order m/m_p all through the shock. This approximation becomes poorer as M approaches unity, and we study the limit in the next section.

3.2.1. Sherman's overshoot

In the Chapman-Enskog theory for binary mixtures used by Sherman (1960) there are also three eigenvalues. For the present limit $m/m_p \rightarrow 0$, $\epsilon = O(1)$, two of them are of order unity for all Mach numbers and the only physically relevant one is of order m/m_p . Remarkably enough, the starting slopes of Sherman's overshooting solution corresponding to this last eigenvalue (which is zero in first approximation, like our λ_3) are equal, in first approximation, to the starting slopes of the outer solution (16) given by (18c, d). These are also the arriving slopes of Sherman's solution at the downstream singular point when M is the downstream Mach number, indicating that the physically relevant eigenvalue in the C-E theory corresponds to our λ_3 for $M > 1$ (though obviously with positive sign) and to λ_2 for $M < 1$. Therefore, for $M_e^2 > 1 + \epsilon$ ($M > 1$) the C-E theory fails to give the correct starting eigenvalue, and produces overshooting solutions. Consequently, even for weak shocks, the C-E theory fails when the heavy component is dilute. It must be noticed that the above identification

of our outer solution and that of Sherman is restricted to the neighbourhood of the singular points, where both approaches agree in depending on some sort of proximity to equilibrium. In fact, out of these regions, both solutions are not the same for the case studied by Sherman.

Apparently, for $M > 1$, the mode absent from the C-E theory and associated to our eigenvalue λ_2 must be connected with our use of two independent momentum conservation equations, rather than only one complemented by a constitutive diffusion law. This is probably the reason why the similar approach of Goldman & Sirovich (1967, 1969) was also free from overshoots. But we cannot be conclusive, as their analysis was restricted to weak shocks, while we have shown that overshoots arise for shocks with $M_e^2 > 1 + \epsilon$. The role played by the two temperatures in this limit is negligible for the approach of Goldman & Sirovich (and for our own), because the temperature of the heavy gas is uncoupled from the problem to first order in m/m_p .

3.3. Solution when $|M^2 - 1| \ll 1$

As $|M^2 - 1|$ becomes small, the thickness of the boundary layer increases and the approximation of the previous section is no longer valid. That this is so is readily seen from the slopes $d\eta/d\xi$ and $d\theta/d\xi$ at $\xi = 1$, which are not $O(F)$. In fact, for $|M^2 - 1| = O(F^{-\frac{1}{2}})$ or smaller, $\lambda_2 = O(F^{-\frac{1}{2}})$ and, from (18)

$$\left. \frac{d\eta}{d\xi} \right|_{\xi=1} = O(F^{\frac{1}{2}}),$$

and similarly for $d\theta/d\xi$ at $\xi = 1$. In particular, for $|M^2 - 1| = O(F^{-1})$, one obtains in first approximation

$$\left. \frac{d\eta}{d\xi} \right|_{\xi=1} = \left(\frac{\sigma F \epsilon}{\sigma + 1 - 1/\gamma} \right)^{\frac{1}{2}}, \quad (20)$$

$$\text{and} \quad \left. \frac{d\theta}{d\xi} \right|_{\xi=1} = (1 - \gamma M^2) \left(\frac{\sigma F \epsilon}{\sigma + 1 - 1/\gamma} \right)^{\frac{1}{2}}. \quad (21)$$

For $|M^2 - 1| \ll 1$ but $|M^2 - 1| \gg F^{-\frac{1}{2}}$, equations (17) are valid and the slopes are $O(|M^2 - 1|F)$.

In the limit $|M^2 - 1| = O(F^{-\frac{1}{2}})$, it can be shown that $\eta - 1 = O(F^{-\frac{1}{2}})$, $\theta - 1 = O(F^{-\frac{1}{2}})$ and $\xi - 1 = O(F^{-1})$ in the boundary layer which, therefore, has a thickness of order F^{-1} . Introducing the variables $\eta^* = (\eta - 1)F^{\frac{1}{2}}$, $\xi^* = (\xi - 1)F$, $\theta^* = (\theta - 1)F^{\frac{1}{2}}$ and

$$\beta = (\gamma - 1)(\eta - 1) + \theta - 1. \quad (22)$$

(14a) may be written as

$$\frac{\gamma \eta^* d\eta^*}{F d\xi^*} = \beta + \frac{\gamma \epsilon \xi^*}{F} - \frac{(\theta^* - \eta^*) \eta^*}{F} [1 + (M^2 - 1)F^{\frac{1}{2}}]. \quad (23)$$

Therefore, at the lowest order we have $\beta = 0$, or

$$\theta - 1 = -(\gamma - 1)(\eta - 1), \quad (24)$$

which states that the light-gas entropy is in first approximation conserved inside the boundary layer.†

† In an earlier version of this paper, the near constancy of β was used as the basis of a stable numerical scheme (see below) without further analysis. Subsequent details of the boundary-layer structure are due to an anonymous referee, including the scaling for η^* , ξ^* and θ^* , and down to (26).

Similarly, (14b) becomes

$$\left(1 + \frac{\gamma-1}{\sigma\gamma}\right) \eta^* \frac{d\eta^*}{d\xi^*} = \frac{1}{2}(\gamma+1) \eta^{*2} + \epsilon \xi^* + \eta^* (M^2 - 1) F^{\frac{1}{2}}. \quad (25)$$

Notice that in writing these equations, terms of order $F^{-\frac{1}{2}}$ have been neglected.

In the limiting case $|M^2 - 1| = O(F^{-1})$, the last term in (25) is small and the solution of this equation that satisfies $\eta^* = 0$ at $\xi^* = 0$ may be written as

$$\eta^{*2} = -\frac{2\epsilon\xi^*}{1+\gamma} - \frac{2\epsilon c}{(1+\gamma)^2} \left\{1 - \exp\left[\frac{(1+\gamma)\xi^*}{c}\right]\right\}, \quad (26)$$

with $c = 1 + (\gamma-1)/\sigma\gamma$. It is easily verified that this solution ((26) in addition to $\theta^* = -(\gamma-1)\eta^*$) correctly yields the slopes (20) at $\xi^* = 0$, and that, in the limit $\xi^* \rightarrow -\infty$, it behaves as the leading term of the outer solution (16) for $\xi \rightarrow 1$ in this limit $|M^2 - 1| = O(F^{-1})$. It has the limitation of holding only for extremely weak light-gas shocks (in He-Xe mixtures, $M^2 - 1$ is equal to F^{-1} for $M = 1.016$). In the more general case $|M^2 - 1| = O(F^{-\frac{1}{2}})$ one has to solve (25) numerically, being forced to carry the expansion to second order as $F^{\frac{1}{2}}$ is not large enough for He-Xe mixtures. Therefore, we choose the alternative procedure of exploiting further the near constancy of β to generate a much more rapidly convergent stable numerical scheme. Combining (14a) and (14b) to form an equation for $d\beta/d\xi$ and retaining only the leading terms in the boundary layer leads to

$$F^{-\frac{1}{2}} \eta^* \frac{d\beta^*}{d\xi^*} = \left(\frac{\gamma-1}{\gamma} + \sigma\right) \beta^* + (\gamma-1) [\epsilon \xi^* + F^{\frac{1}{2}} (M^2 - 1) \eta^* + \eta^{*2} (1 - \frac{1}{2}\sigma\gamma)], \quad (27)$$

with $\beta^* = \beta F = O(1)$. Therefore, because $\beta^* = F^{\frac{1}{2}} [\theta^* + (\gamma-1)\eta^*]$ the algebraic equation $\theta^* = \theta^*(\eta^*, \xi^*)$ which results from equating to zero the right-hand side of (27), has errors of order F^{-1} in the boundary layer, rather than $O(F^{-\frac{1}{2}})$ as in the equation $\theta^* = -(\gamma-1)\eta^*$. This result can be generalized through the entire shock wave, since in the outer region, the algebraic equation resulting from making $d\beta/d\xi = 0$ by combining (14a, b), is a linear combination of (16) and, thus, has errors $O(F^{-1})$.

Hence, the expression

$$(\gamma-1) \left[(\eta-1) + \epsilon(\xi-1) + \frac{1}{\gamma M^2} \left(\frac{\theta}{\eta} - 1 \right) \right] + \frac{2}{3} P \gamma (\gamma-1) M^2 \left\{ -(\eta-1)^2 + \epsilon(\xi-1)(\xi-2\eta+1) + \frac{2}{\gamma(\gamma-1)M^2} [\theta + (\gamma-1)\eta - \gamma] \right\} = 0, \quad (28)$$

is, with errors $O(F^{-1})$, an integral of the equations in the limit $M^2 - 1 \ll 1$ which, in addition to either (14a) or (14b) (in subsequent calculations we shall use (14a)) gives the solution in phase space. The order of the system is reduced from third to second, eliminating the eigenvalue λ_1 which made the numerical integration unstable. With respect to the boundary-layer equation (25), this procedure has the advantage that with the same amount of numerical work (the integration of an ordinary first-order differential equation) one obtains the solution through the whole shock (rather than only in the boundary layer) with errors $O(F^{-1})$ (rather than $O(F^{-\frac{1}{2}})$), and without a need for matching the inner and outer solutions (except in the very narrow limit $M^2 - 1 = O(F^{-1})$ governed by the analytical solution (26) in the boundary layer, with errors of order $F^{-\frac{1}{2}}$).

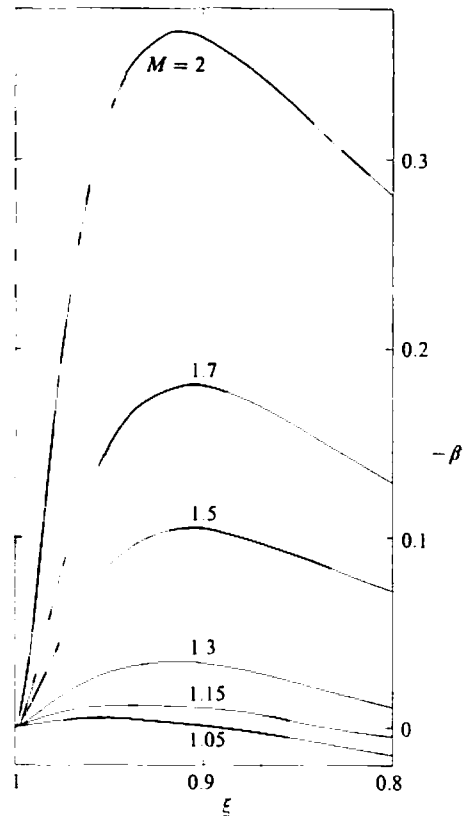


FIGURE 4. β' -function [equation (22a)] for some values of M (He-Xe, $\epsilon = 0.5$). Numerical values used are $m_v/m = 32.75$; $Pr = 0.67$; $Sc = 2.30$.

An improved definition of the quantity β , such that $d\beta/d\xi = 0$ at $\xi = 1$, may be given as

$$\beta' = A(\eta - 1) + \theta - 1, \quad (22')$$

where A is the exact slope $[-d\theta/d\eta]_{\eta=1}$ corresponding to the eigenvalue λ_2 :

$$A = \gamma M^2(1 - \lambda_2) - 1 + \frac{\epsilon \gamma M^2}{1 + \lambda_2 F} = \gamma - 1 + O(F^{-1}) + O\left(\frac{|M^2 - 1|}{M^2}\right).$$

With this new definition of β' , the corresponding 'integral of the motion' would be obtained by replacing the leading $(\gamma - 1)$ term by A in (28). As an indication of self-consistency of this approximate method of solution, figure 4 shows the variable β' so calculated as a function of ξ . It is observed that β' is of the same order as ξ all through the shock, even for values of $|M^2 - 1|/M^2$ that are not so small. The shock-wave structures obtained by this method are shown in figure 5 in phase space, for a He-Xe mixture with $\epsilon = 0.5$, and for $M = 0.95$ and $M = 1.15$; we also include a comparison with the corresponding outer solution. (For $M < 1$ both curves are practically the same.)

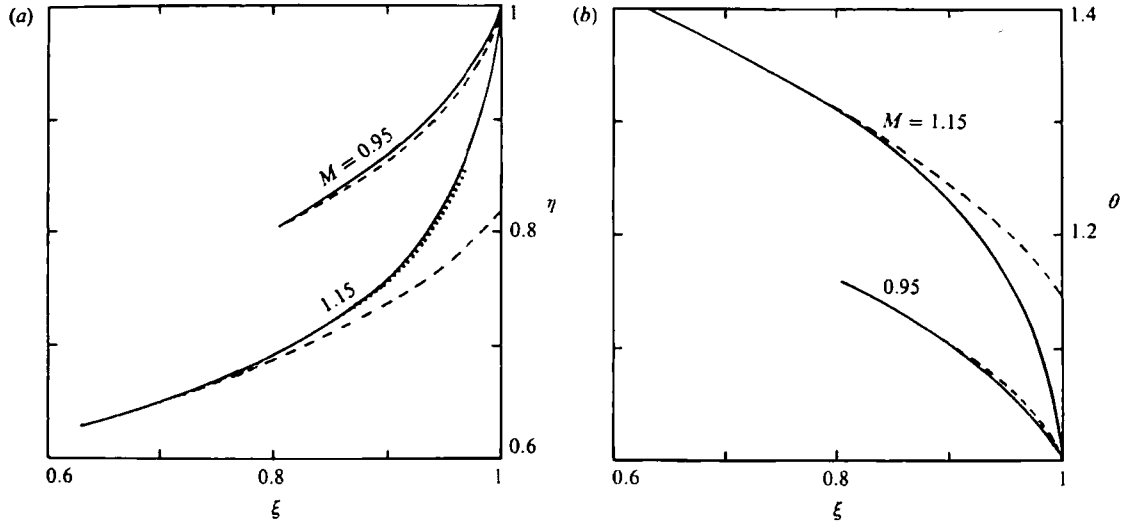


FIGURE 5. Numerical results for the structure of the shock compared to the outer solution for $M = 0.95$ and $M = 1.15$ (He-Xe, $\epsilon = 0.5$). The dotted line in figure 4(a) corresponds to a higher-order outer solution (§3.4).

3.4. Higher-order approximations for the outer solution

It is relatively simple to obtain successive corrections for the outer solution. To this end, we solve (14) for η and θ , obtaining

$$\eta = 1 + \frac{1}{\gamma + 1} \left\{ \left(\frac{1 - M^2}{M^2} - \gamma \epsilon (\xi - 1) + \Delta_1 \right) - \left[\left(\frac{1 - M^2}{M^2} - \gamma \epsilon (\xi - 1) + \Delta_1 \right)^2 + (\gamma + 1) (\epsilon (\gamma - 1) (\xi - 1)^2 + 2\Delta_1 - 2\epsilon (\xi - 1) - (\gamma - 1)\Delta_2) \right]^{\frac{1}{2}} \right\}, \quad (29a)$$

$$\theta = \eta + \gamma M^2 \eta [\Delta_1 - (\eta - 1) - \epsilon (\xi - 1)], \quad (29b)$$

where

$$\Delta_1 = \frac{\eta - \xi}{\eta \theta^{-1} \xi} \frac{1}{F} \frac{d\eta}{d\xi},$$

and

$$\Delta_2 = \frac{3}{2Pr(\gamma - 1)M^2} \frac{\eta - \xi}{\eta \xi \theta^{-1}} \frac{1}{F} \frac{d\theta}{d\xi}.$$

In first approximation we make $\Delta_1 = \Delta_2 = 0$ to obtain (16a) and (16b) ($\eta_0 = \eta_0(\xi)$, $\theta_0 = \theta_0(\xi)$). Using these expressions to evaluate Δ_1 and Δ_2 for each ξ and introducing them into (29), the second-order approximation $\eta_1 = \eta_1(\xi)$ and $\theta_1 = \theta_1(\xi)$ is obtained, and so on. Carrying out these corrections, one finds that they become smaller and the convergence is faster as M increases (for a He-Xe mixture with $\epsilon = 0.5$, the larger corrections are about 2% of the first-order approximation for $M = 2$, and the first correction contains 99.99% of the total correction). When M is very near unity (where the first-order outer solution is a poor approximation to the solution) the corrections are important, and the outer solution does converge to a curve practically indistinguishable from the integrated solution obtained by the method of §3.3, as shown in figure 5 for the velocity profile in the case of $M = 1.15$. However, the procedure becomes unstable for M near unity in the neighbourhood of $\xi = 1$

and we have not succeeded in obtaining the complete shock structure from this iterative approach.

Finally, it is worth pointing out that a similar procedure can be used to obtain higher-order approximations to the solution given in §3.3 for M near unity: from the first approximation we can calculate (numerically) $d\beta/d\xi$ using (14) for each ξ and use it to improve the algebraic relation (28); with the new solution, $d\beta/d\xi$ can be calculated again, and so on. The difference is that the above procedure can be carried out algebraically while this must be made numerically.

3.5. Structure of the boundary layer when $M^2 - 1 = O(1)$ or larger

To obtain the boundary-layer structure (light-gas shock wave as a pure gas), one puts $\xi = 1$ in (14) and the resulting first-order differential equation $d\eta/d\theta = G(\theta, \eta)$ is solved with the boundary conditions (15a) (upstream) and (15c, d) (downstream). As is well known (i.e. Millán 1975), to avoid the numerical instabilities at the upstream singular point (15a) (a node), one must start the integration from the downstream saddle point. Yet, the results of this analysis must be interpreted carefully because the equilibrium closure used for the light gas fails within the internal shock wave except for weak shocks. Keeping such a limitation in mind, Riesco-Chueca *et al.* (1986) have considered the structure of this boundary layer to the next order, discovering a singularity at the point θ_1, η_1 (downstream conditions of the pure light-gas shock). There, an interesting new intermediate boundary layer arises that admits a linear treatment and may thus be described analytically. The corresponding exponential solutions decay downstream towards the outer solution and grow unstably in the upstream direction to merge with the sharp pure light gas shock. The analysis is not completely devoid of physical interest because the near equilibrium closure for the light gas is still valid in the vicinity of the point θ_1, η_1 .

4. Limitations of the present model

In deriving the shock equations in §2 the following hypotheses were used: (i) the heavy-gas partial pressure, internal energy and heat flux are neglected in the mixture equations (3) and (4); (ii) the heavy gas is assumed to be in hypersonic conditions in its momentum conservation equation; (iii) a linear dependence of the momentum transfer on the slip velocity has been used (equation (7)), and finally (iv) a hydrodynamical closure is used for the light gas (equation (5)). The first of these hypotheses (i), is a direct consequence of the small molar fraction of the heavy species [of order $m/m_p \epsilon = O(m/m_p)$] and is the only one that affects the phase-space outer solution developed in §3.1. Moreover, except near $\xi = 1$, this outer solution in phase space is valid for strong shock waves, despite the fact that hydrodynamical equations for the light gas have been used, and despite the linear drag relaxation law (7) (which is less accurate as the shock becomes stronger), because neither (5) for the flux laws nor (7) for the relaxation law were needed. These relations were used, however, for deriving the phase-space solution in §3.3 for shocks with M close to unity, in which case both are rather good assumptions. In this phase-space solution for Mach numbers near unity, the (more restrictive) hypersonic hypothesis is also used and it is convenient to give a quantitative criterion for its validity: the heavy-species velocity must be much larger than its sound speed downstream of the shock,

$$u_2^2 \gg \frac{\gamma k T_2}{m_p}$$

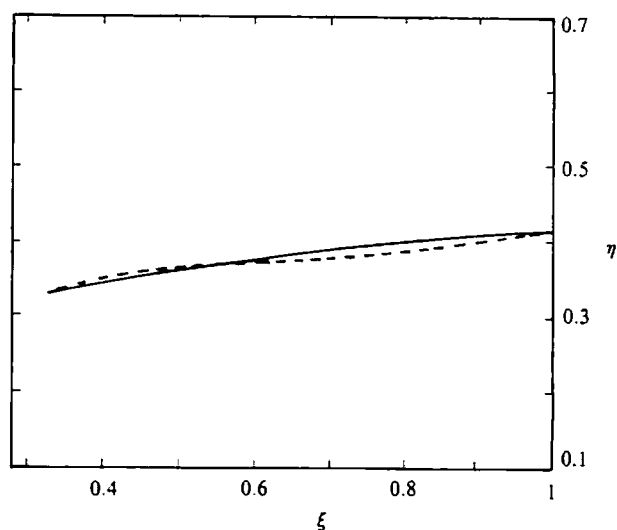


FIGURE 6. Outer solution for the velocity (—) compared with results by Harris & Bienkowski (1970) (----) (He-Xe mixture, $\epsilon = 1$, $M = 2.12$).

or in terms of the dimensionless variables,

$$M_2^2 \equiv M^2 \frac{\eta_2^2}{\theta_2} \gg \frac{m}{m_p}, \quad (30)$$

where the left-hand side of the inequality is the downstream light-gas Mach number, which must be very large compared to the mass ratio for the hypersonic hypothesis to be reasonable. Using (15*b*), we can write the above inequality in the form $G(M, \epsilon) \gg m/m_p$, where the function $G(M, \epsilon)$ is plotted in figure 7. As seen in this figure, the restriction becomes more stringent for strong shocks (as M goes to infinity, G goes to $(\gamma - 1)/2\gamma(1 + \epsilon)$) and for increasing values of the density ratio ϵ . In this condition (30) it is implicit that the highest heavy-gas temperature is reached in the downstream region. However, it has been shown (Harris & Bienkowski 1971; Bird 1984) that the parallel temperature (xx -component of the temperature tensor) of the heavy gas has an overshoot over the downstream value, and thus it is this maximum in the temperature which must be considered. Hence, a complete self-consistency check would require following the heavy-gas temperature equations along the shock, which can be done by means of the hypersonic closure (see Harris & Bienkowski 1971; Fernández de la Mora 1985). As shown by Bird (1984) and Riesco-Chueca *et al.* (1986), the overshoot grows, with the Mach number reaching an asymptotic value which depends on ϵ and m_p/m . Typically, for He-Xe mixtures and $\epsilon = 1$, this asymptotic value is $T_{xx}/T_2 \sim 1.5$. Therefore, condition (30) is only slightly modified.

With respect to the linear expression for the momentum transfer between species, it is clear that, for strong shocks, a more realistic law must be used because the slip velocity is no longer small (Riesco-Chueca *et al.* 1986, 1987). As discussed earlier in this section, this hypothesis does not affect the outer solution in phase space and this is the reason why our first-order results in phase space are practically the same as the zero-order solution of Harris & Bienkowski (1971) in the limit $m/m_p \ll 1$, $\epsilon = O(1)$ (see figure 6), in spite of their use of Maxwell molecules. To obtain this solution, these authors skipped the numerical instability discussed by Sirovich & Goldman (1969).

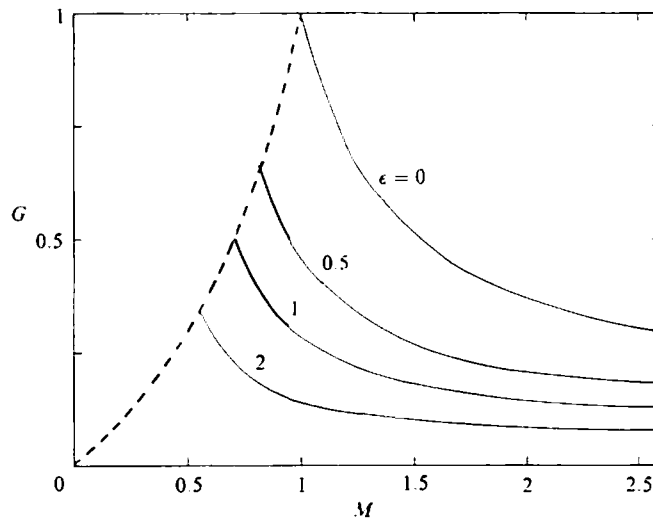


FIGURE 7. Function $G(M, \epsilon)$ [left-hand side of inequality (25)]. The hypersonic assumption remains valid even on the hot side of the wave provided $G \gg m/m_p$.

by starting the integration at the downstream conditions of the inner shock of the light gas (intersection point of the outer solution with the axis $\xi = 1$ in figure 1). However, they did not consider the case where the inner shock is very weak, in which their expansion in powers of m/m_p does not remain valid.

5. Comparison with experiments

The seminal experiments of Gmurczyk *et al.* (1979), revealing a rich variety of shock structures in He-Xe mixtures (double humps, two scales, etc.), motivated a new stream of papers on the subject, which has proceeded independently from the dusty-gas literature and the paper of Harris & Bienkowski. More recently, these authors (Tarczynski *et al.* 1986) have refined a slight inaccuracy in the downstream tail of their former shock-tube data, and have also presented new experiments on shocks in free jets. These later data will not be compared with our results here because, at the low Reynolds numbers prevailing at the nozzle, the upstream shock conditions are removed from equilibrium.

Figure 8 contains a comparison between our phase-space results and the 1986 shock-tube experiments corresponding to the smallest heavy-gas molar fraction (3% Xe or $\epsilon = 1.015$): one for a weak shock ($M = 1.09$) in which the solution of §3.3 may be applied, and another one for a strong shock ($M = 3.09$) for which the phase-space solution is given by the outer solution (16). The agreement is excellent in both cases. Riesco-Chueca *et al.* (1986) have compared real-space results from the present model against experiments by Gmurczyk *et al.* (1979), also with fairly good agreement in the location of the first hump and the shock width. This fact provides strong support for our governing equations which connect phase-space and real-space structures unequivocally once the light-gas viscosity is specified.

It is a pleasure to thank Dr Antonio Barrero (Sevilla), Dr Antonio Vázquez (MIT), Pascual Riesco-Chueca (Yale) and Drs Herczynski and Walenta (Warsaw) for their useful remarks on this manuscript.

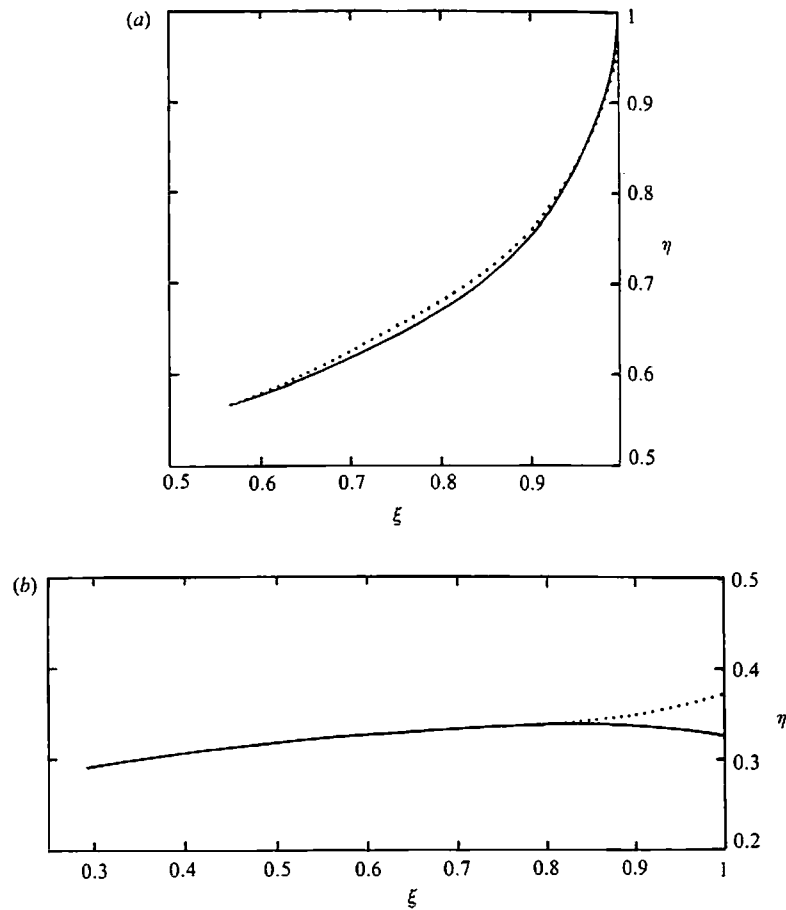


FIGURE 8. Comparison with shock-tube experiments for He-Xe mixtures of Tarczyński *et al.* (1986). The continuous curves correspond to phase-space ($\eta-\xi$) theoretical results and the broken curves to experiments. In figure 8(a), $M = 1.09$, $\epsilon = 1.015$ ($M_e = 1.54$, 3% molar fraction of Xe) and the theoretical curve is calculated using the function β' . Figure 8(b) corresponds to $M = 3.09$, $\epsilon = 1.015$ ($M_e = 4.38$, 3% molar fraction of Xe), with the outer solution (16) as the continuous line.

The present work has been supported in part by the 'Junior Faculty Fellowship' of Yale University as well as a cooperative research grant from Schmitt Technologies Associates and the State of Connecticut (number 885-176). In its initial stages, this research was supported by the National Science Foundation Grant CPE-88205378.

REFERENCES

- BIRD, G. A. 1968 *J. Fluid Mech.* **31**, 657.
 BIRD, G. A. 1984 Shock wave structure in gas mixtures. In *Rarefied Gas Dynamics* (ed. H. Oguchi), vol. 1, p. 175. University of Tokyo Press.
 BRATOS, M. & HERCZYŃSKI, R. 1980 *Bull. Acad. Pol. Sci.* **28**, 259.
 BRATOS, M. & HERCZYŃSKI, R. 1983 The shock wave structure in one-component gas and in binary gas mixtures. *Prace IPPT-IFTR reports* 19/1983.
 BURGERS, J. M. 1969 *Flow Equations for Composite Gases*. Academic.
 CARRIER, G. F. 1958 *J. Fluid Mech.* **4**, 376.

- CENTER, R. E. 1967 *Phys. Fluids* **10**, 1777.
- COWLING, T. G. 1942 *Phil. Mag.* **33**, 61.
- DYAKOV, S. P. 1954 *Zh. Eksp. Theor. Fiz.* **27**, 728.
- FERNÁNDEZ DE LA MORA, J. 1984 *J. Phys. Chem.* **88**, 4557.
- FERNÁNDEZ DE LA MORA, J. 1985 *J. Chem. Phys.* **82**, 3453.
- FERNÁNDEZ DE LA MORA, J. & FERNÁNDEZ-FERIA, R. 1987 Kinetic theory of gas mixtures with large mass disparity. *Phys. Fluids* **30**, 740.
- FERNÁNDEZ DE LA MORA, J., WILSON, J. A. & HALPERN, B. L. 1984 *J. Fluid Mech.* **149**, 217.
- GMURCZYK, A. S., TARCZYNSKI, M. & WALENTA, Z. A. 1979 Shock wave structure in the binary mixtures of gases with disparate molecular masses. In *Rarefied Gas Dynamics* (ed. R. Campargue), vol. 1, pp. 333-341. Commissariat à l'Énergie Atomique, Paris.
- GOLDMAN, E. & SIROVICH, L. 1967 *Phys. Fluids* **10**, 1928.
- GOLDMAN, E. & SIROVICH, L. 1969 *J. Fluid Mech.* **33**, 575.
- HAMAD, H. & FROHN, A. 1980 *Z. angew. Math. Phys.* **31**, 66.
- HARRIS, W. L. & BIENKOWSKI, G. K. 1970 Asymptotic theory of the structure of normal shock waves in binary gas mixtures. *Princeton Univ. Dept. Aerospace and Mech. Sci. Rep.* no. 985.
- HARRIS, W. L. & BIENKOWSKI, G. K. 1971 *Phys. Fluids* **14**, 2652.
- MAISE, G. & FENN, J. B. 1972 *Trans. ASME C: J. Heat Transfer* **94**, 29.
- MARBLE, F. E. 1970 *Ann. Rev. Fluid Mech.* **2**, 397.
- MILLÁN, G. 1975 Problemas matemáticos de la mecánica de fluidos. Estructura de las ondas de choque y Combustión, p. 356. Madrid, Royal Academy of Sciences.
- PLATKOWSKI, T. 1979 Application of the modified BGK equations to the shock wave structure in disparate mass mixtures. In *Rarefied Gas Dynamics* (ed. R. Campargue), vol. 1, pp. 323-341. Commissariat à l'Énergie Atomique, Paris.
- REIS, V. H. & FENN, J. B. 1963 *J. Chem. Phys.* **39**, 3240.
- RIESCO-CHUECA, P., FERNÁNDEZ-FERIA, R. & FERNÁNDEZ DE LA MORA, J. 1986 Nonlinearities in the interspecies transfer of Momentum and Energy for disparate-mass gas mixtures and shock wave structure. In *Rarefied Gas Dynamics* (ed. V. Boffi & C. Cercignani), Vol. 1, p. 283. Stuttgart: Teubner.
- RIESCO-CHUECA, P., FERNÁNDEZ-FERIA, R. & FERNÁNDEZ DE LA MORA, J. 1987 *Phys. Fluids* **30**, 45.
- SCHMIDT, B., SEILER, F. & WÖRNER, M. 1984 *J. Fluid Mech.* **143**, 305.
- SCHWARTZ, M. H. & ANDRES, R. P. 1977 *Rarefied Gas Dynamics* (ed. J. L. Potter), pp. 135-149. AIAA Prog. Astronautics Aeronautics, vol. 5.
- SHERMAN, F. S. 1960 *J. Fluid Mech.* **8**, 465.
- SIROVICH, L. & GOLDMAN, E. 1969 Normal shock structure in a binary gas. In *Rarefied Gas Dynamics* (ed. L. Trilling & N. Y. Wachmann), vol. 1, pp. 407-415. Academic.
- SRIVASTAVA, R. S. & ROSNER, D. E. 1979 *Intl J. Heat Mass Transfer* **22**, 1281.
- SRIVASTAVA, R. S. & SHARMA, J. P. 1982 *Z. angew. Math. Phys.* **33**, 818.
- TARCZYNSKI, M., HERCZYNSKI & WALENTA, Z. A. 1986 *Shock Tube Symposium*. Stanford (in press).
- THUAN, N. K. & ANDRES, R. P. 1979 *11th Symp. on Rarefied Gas Dynamics* (ed. R. Campargue), vol. 1, pp. 667-682. Commissariat à l'Énergie Atomique, Paris.